

# Matching Pursuit LASSO Part II: Applications and Sparse Recovery over Batch Signals

Mingkui Tan, Ivor W. Tsang, and Li Wang

**Abstract**—In Part I [1], a Matching Pursuit LASSO (MPL) algorithm has been presented for solving large-scale sparse recovery (SR) problems. In this paper, we present a subspace search to further improve the performance of MPL, and then continue to address another major challenge of SR – batch SR with many signals, a consideration which is absent from most of previous  $\ell_1$ -norm methods. As a result, a batch-mode MPL is developed to vastly speed up sparse recovery of many signals simultaneously. Comprehensive numerical experiments on compressive sensing and face recognition tasks demonstrate the superior performance of MPL and BMPL over other methods considered in this paper, in terms of sparse recovery ability and efficiency. In particular, BMPL is up to 400 times faster than existing  $\ell_1$ -norm methods considered to be state-of-the-art.

**Index Terms**—Batch mode LASSO, sparse recovery, big dictionary, compressive sensing, face recognition.

## I. INTRODUCTION

With the fast development of compressive sensing theory [2], sparse recovery (SR) has gained increased attention recently in the signal processing community [2], [3], [4], [5]. It has also become a fundamental element of many other research areas, such as image processing, computer vision, data mining and machine learning [6], [7], [8], [9], [10], [11].

Formally, SR seeks to recover an unknown  $k$ -sparse signal  $\mathbf{x} \in \mathbb{R}^m$  from its nonadaptive linear measurement  $\mathbf{b} = \mathbf{A}\mathbf{x} + \mathbf{e} \in \mathbb{R}^n$ , where  $\mathbf{A} \in \mathbb{R}^{n \times m}$  ( $n \ll m$ ) denotes the dictionary,  $\mathbf{e} \in \mathbb{R}^n$  represents the noise, and each column vector of  $\mathbf{A}$  is referred to as an atom. To recover  $\mathbf{x}$  from  $\mathbf{b}$ , one need to solve an  $\ell_0$ -norm minimization problem:

$$\min_{\mathbf{x}} \|\mathbf{x}\|_0, \quad \text{s.t. } \mathbf{b} = \mathbf{A}\mathbf{x}, \quad (1)$$

where  $\|\cdot\|_0$  denotes the  $\ell_0$ -norm of a vector. Problem (1) is NP-complete [12], [2], [13], and many researchers propose to solve its  $\ell_1$ -convex relaxations instead [14], [15], [3], such as the following LASSO problem [16], [17], [18], [19]:

$$\min_{\mathbf{x}} \lambda \|\mathbf{x}\|_1 + \frac{1}{2} \|\mathbf{b} - \mathbf{A}\mathbf{x}\|^2, \quad (2)$$

where  $\lambda$  is a regularization parameter. Regarding problem (2), many methods have been proposed over the last decade,

such as the least-angle regression (LARS) [20], gradient projection for sparse reconstruction (GPSR) [17], projected gradient (PG) [21], fast iterative shrinkage-threshold algorithm (FISTA) [22], coordinate descent methods [23], proximal gradient homotopy (PGH) method [18], [19] and so on. Interested readers can refer to Part I and the references therein [1] for a more comprehensive review.

Existing  $\ell_1$ -norm methods, however, suffer from high computational complexity for large-scale SR problems. More critically, for problems like *batch SR* [24], in which many signals need to be sparsely recovered simultaneously, the computations will be even more expensive. Here, the batch SR problem is carried out to solve the following optimization problem:

$$\min_{\mathbf{X}} \|\mathbf{B} - \mathbf{A}\mathbf{X}\|_F^2 + \lambda \sum_{i=1}^p \|\mathbf{x}_i\|_1, \quad (3)$$

where  $\mathbf{B} = [\mathbf{b}_1, \dots, \mathbf{b}_p] \in \mathbb{R}^{n \times p}$  records the measurements of  $p$  signals and  $\|\cdot\|_F$  denotes the  $F$ -norm of a matrix. The batch SR problem plays an important role in many applications, such as face recognition [7], [25], compressive sensing [26], [27], dictionary learning [28], [29] and so on.

### A. Batch SR in Face Recognition

Face recognition by SR has achieved promising performance recently [7], [25], [30], [31], [32]. The basic assumption is that, any testing image lies in a subspace spanned by the training images of a person [7], [33], [25], thus it can be sparsely represented by the training images. Here, the training images are formed as a dictionary  $\mathbf{A} \in \mathbb{R}^{n \times m}$ , where  $n$  denotes the number of pixels or features of a face image, and  $m$  denotes the number of training images. The core task of SR based face recognition is to find a sparse representation of a testing image  $\mathbf{b}$  over  $\mathbf{A}$ . However, directly solving problem (2) is computationally expensive especially when  $n$  is very large [7], [33], [25]. Some researchers propose to reduce the computational cost by dimension reduction methods, such as random projections [7]. However, the recognition rates may be affected due to the dimension reduction [33], [25], [10].

In practice, it is often required to recognize many face images simultaneously in real-time, which is very challenging for SR based methods [33], [34]. To address this, the authors in [33] suggest directly solving  $\min_{\mathbf{x}} \frac{1}{2} \|\mathbf{b} - \mathbf{A}\mathbf{x}\|^2$ , which is denoted by L2; while the authors in [34] argue that solving a least square problem  $\min_{\mathbf{x}} \frac{1}{2} \|\mathbf{b} - \mathbf{A}\mathbf{x}\|^2 + \frac{\lambda}{2} \|\mathbf{x}\|^2$ , which is denoted by L2-L2, can achieve more stable performance. For the L2 method, the optimal solution is  $\mathbf{x}^* = \mathbf{R}^+ \mathbf{Q}^T \mathbf{b}$ ,

Mingkui Tan is with the School of Computer Science, the University of Adelaide, Australia. e-mail: mingkui.tan@adelaide.edu.au.

Ivor W. Tsang is with the Centre for Quantum Computation & Intelligent Systems (QCIS), at the University of Technology, Sydney (UTS), Australia. e-mail: Ivor.Tsang@uts.edu.au.

Li Wang is with the Institute for Computational and Experimental Research in Mathematics (ICERM), Brown University, USA. e-mail: liwangucsd@gmail.com.

where  $\mathbf{A} = \mathbf{Q}\mathbf{R}$  denotes the QR decomposition of  $\mathbf{A}$ , and  $\mathbf{R}^+$  denotes the pseudo inverse. For the L2-L2 method, the optimal solution is  $\mathbf{x}^* = (\mathbf{A}^\top \mathbf{A} + \lambda \mathbf{I})^{-1} \mathbf{A}^\top \mathbf{b}$ . Therefore, fast predictions can be achieved via simple matrix-vector products by pre-computing  $\mathbf{R}^{-1} \mathbf{Q}^\top$  and  $(\mathbf{A}^\top \mathbf{A} + \lambda \mathbf{I})^{-1}$  off-line. However, since the solutions of the two methods are not sparse, the recognition performance may be degraded.

### B. Batch SR in Compressive Sensing

Sparse recovery is a core element of the recently developed compressive sensing theory on signal acquisition [2]. In compressive sensing, a signal is allowed to be captured at a rate significantly lower than the Nyquist rate, if it is compressible or can be sparsely decomposed under a basis  $\Psi = [\Psi_1, \dots, \Psi_m] \in \mathbb{R}^{m \times m}$  [3], [26]. To recover the original signal, we need to solve a sparse recovery problem [26], [27], which might be very expensive. Moreover, in real-world sensing tasks, such as imaging and video sensing [27], [35], it is often necessary to sense a large number of signals simultaneously in real-time. Therefore, it is critical to efficiently address the large-scale batch SR problem in compressive sensing.

### C. Batch SR in Dictionary Learning

Dictionary learning, which aims to find a good dictionary based on a set of training signals, has recently become increasingly important in many areas, such as signal processing, computer vision and machine learning [29], [24], [36], [37], [38]. To learn a good dictionary, many training examples (or signals) are usually required to be sparsely represented at the same time, leading to an intolerable cost for dictionary learning. The large-scale batch SR problem therefore is a core step in dictionary learning [29], [36].

### D. Main Contributions

In Part I of this paper, we have presented a matching pursuit LASSO (MPL) algorithm in relation to the computational issues of LASSO over big dictionaries. In this paper, we first present a subspace search to further improve the performance of MPL, and then continue to address the computational bottleneck created by the batch SR problem. The main contributions of this paper are summarized as follows:

- A subspace exploratory matching is proposed to improve the performance of MPL. This new matching pursuit scheme takes less than 50 seconds to recover a 600-sparse signal over a dictionary of one million atoms.
- A batch mode MPL (BMPL), which is absent in many  $\ell_1$ -norm methods, is presented to address large-scale batch SR problems.
- We apply BMPL to face recognition tasks on two well-known face databases, namely *Extended YaleB* and *AR* databases. Comprehensive experiments show that BMPL achieves comparable or better recognition rates than baselines with comparable time complexity. Importantly, BMPL is up to 400 times faster than existing  $\ell_1$ -norm methods considered to be state-of-the-art.

The rest of this paper is organized as follows. In Section II, we briefly review the MPL algorithm and then propose an improved MPL algorithm with subspace exploratory matching. In Section III, we describe the batch mode MPL method. Numerical experiments and real-world applications are presented in Sections IV and V, respectively. Conclusive remarks are given in Section VI.

## II. MATCHING PURSUIT FOR LASSO

Throughout the paper, we denote the transpose of a vector/matrix by the superscript  $^\top$ ,  $\mathbf{0}$  as a zero vector and  $\text{diag}(\mathbf{v})$  as a diagonal matrix with diagonal entries equal to  $\mathbf{v}$ . In addition, let  $\|\mathbf{v}\|_p$  and  $\|\mathbf{v}\|$  denote the  $\ell_p$ -norm and  $\ell_2$ -norm of a vector  $\mathbf{v}$ , respectively. For a function  $f(\mathbf{x})$ , let  $\nabla f(\mathbf{x})$  and  $\partial f(\mathbf{x})$  be the gradient and subgradient of  $f(\mathbf{x})$  at  $\mathbf{x}$ , respectively. For a sparse vector  $\mathbf{x}$ , let the calligraphic letter  $\mathcal{T} = \text{support}(\mathbf{x}) = \{i | x_i \neq 0\} \subset \{1, \dots, m\}$  be its support,  $\mathbf{x}_{\mathcal{T}}$  be the subvector indexed by  $\mathcal{T}$ , and  $\mathcal{T}^c$  be the complementary set of  $\mathcal{T}$ , i.e.  $\mathcal{T}^c = \{1, \dots, m\} \setminus \mathcal{T}$ . Furthermore, let  $\mathbf{A} \odot \mathbf{B}$  represent the element-wise product of two matrices  $\mathbf{A}$  and  $\mathbf{B}$ . Lastly, let  $\mathbf{A}_{\mathcal{T}}$  denote the columns of  $\mathbf{A}$  indexed by  $\mathcal{T}$ .

### A. Matching Pursuit LASSO

To introduce MPL, in [1], we bring in a support detection vector  $\boldsymbol{\tau} \in \{0, 1\}^m$  to  $\mathbf{x}$ , and impose an  $\ell_0$ -norm constraint on  $\boldsymbol{\tau}$ , namely  $\|\boldsymbol{\tau}\|_0 \leq \varrho$ , to enforce the sparsity. Here,  $\varrho$  is a predefined integer satisfying  $1 \leq \varrho < k$ .<sup>1</sup> Let  $\Lambda = \{\boldsymbol{\tau} : \|\boldsymbol{\tau}\|_0 \leq \varrho, \boldsymbol{\tau} \in \{0, 1\}^m\}$  be the domain of  $\boldsymbol{\tau}$ , we propose to solve an integer programming model of LASSO:

$$\begin{aligned} \min_{\boldsymbol{\tau} \in \Lambda} \min_{\mathbf{x}, \boldsymbol{\xi}} \quad & \lambda \|\mathbf{x}\|_1 + \frac{1}{2} \|\boldsymbol{\xi}\|^2 \\ \text{s.t.} \quad & \boldsymbol{\xi} = \mathbf{b} - \mathbf{A}(\mathbf{x} \odot \boldsymbol{\tau}). \end{aligned} \quad (4)$$

Rather than solving this problem directly, we bring in dual variables  $\boldsymbol{\alpha} \in \mathbb{R}^n$  to the constraint  $\boldsymbol{\xi} = \mathbf{b} - \mathbf{A}(\mathbf{x} \odot \boldsymbol{\tau})$  w.r.t. any fixed  $\boldsymbol{\tau}$ , and transform (4) into a minimax problem by introducing the dual form of the inner problem in (4):

$$\begin{aligned} \min_{\boldsymbol{\tau} \in \Lambda} \max_{\boldsymbol{\alpha} \in \mathbb{R}^n} \quad & -\frac{1}{2} \|\boldsymbol{\alpha}\|^2 + \boldsymbol{\alpha}^\top \mathbf{b} \\ \text{s.t.} \quad & \|\boldsymbol{\alpha}^\top \mathbf{A} \text{diag}(\boldsymbol{\tau})\|_\infty \leq \lambda. \end{aligned} \quad (5)$$

Let

$$f(\boldsymbol{\alpha}, \boldsymbol{\tau}) = \frac{1}{2} \|\boldsymbol{\alpha}\|^2 - \boldsymbol{\alpha}^\top \mathbf{b}, \quad \boldsymbol{\alpha} \in \mathcal{A}_{\boldsymbol{\tau}}^\lambda,$$

where  $\mathcal{A}_{\boldsymbol{\tau}}^\lambda = \{\boldsymbol{\alpha} : \|\boldsymbol{\alpha}^\top \mathbf{A} \text{diag}(\boldsymbol{\tau})\|_\infty \leq \lambda, \boldsymbol{\alpha} \in [-l, l]^n\}$  denotes the domain of  $\boldsymbol{\alpha}$  w.r.t. a feasible  $\boldsymbol{\tau}$ , and  $l > 0$  is a large number. By applying a convex relaxation to (5), MPL seeks to solve the following convex problem:

$$\min_{\boldsymbol{\alpha} \in \mathbb{R}^n, \theta \in \mathbb{R}} \theta, \quad \text{s.t.} \quad f(\boldsymbol{\alpha}, \boldsymbol{\tau}) \leq \theta, \quad \forall \boldsymbol{\tau} \in \Lambda. \quad (6)$$

The details of MPL are presented in Algorithm 1. Basically, it iteratively adds a set of active atoms by worst-case analysis in Step 3, and conducts a master problem optimization in Steps 4-8. Let  $\mathbf{g} = \mathbf{A}^\top \boldsymbol{\alpha}^{t-1}$  and  $\mathcal{I}_t$  be the index set of the detected atoms at the  $t$ th iteration, the worst-case analysis is to update

<sup>1</sup>Interested readers may find more discussions of  $\varrho$  in Part I [1].

$\mathcal{I}_t$  based on  $\mathbf{g}$ . We find the  $\varrho$  atoms with the largest  $|g_j|$ , and then record their indices into  $\mathcal{J}_t$ . After that, we update  $\mathcal{I}_t$  by  $\mathcal{I}_t = \mathcal{I}_{t-1} \cup \mathcal{J}_t$ . The master problem optimization from Steps 4-8 is to solve the following problem:

$$\min_{\mathbf{x}, \boldsymbol{\xi}} \lambda \|\mathbf{x}\|_1 + \frac{1}{2} \|\mathbf{b} - \mathbf{A}\mathbf{x}\|^2, \text{ s.t. } \mathbf{x}_{\mathcal{I}_t^c} = \mathbf{0}. \quad (7)$$

The proximal gradient (PG) [21] (resp. conjugate gradient descent (CGD) [39]) is adopted to solve (7) when  $\lambda > 0$  (resp.  $\lambda = 0$ ), as shown in the inner **for loop**. For the **for loop**, to distinguish it from the outer **while loop**, we use  $\mathbf{u}$  as variables.

---

**Algorithm 1** Matching Pursuit Lasso for Solving (6)

---

- 1: Initialize  $\mathbf{x}^0 = \mathbf{0}$ ,  $\boldsymbol{\xi}^0 = \mathbf{b}$ ,  $\mathcal{I}_0 = \emptyset$ . Let  $t = 1$ .
  - 2: **while** (The stopping condition is not achieved) **do**
  - 3:   Do worst-case analysis:  
       Let  $\mathbf{g} = \mathbf{A}^\top \boldsymbol{\alpha}^{t-1}$ ; choose the  $\varrho$  largest  $|g_j|$  and record their indices in  $\mathcal{J}_t$ ; let  $\mathcal{I}_t = \mathcal{I}_{t-1} \cup \mathcal{J}_t$ .
  - 4:   Initialize  $\mathbf{u}_{\mathcal{I}_t}^0 = \mathbf{x}_{\mathcal{I}_t}^{t-1}$  and  $\mathbf{u}_{\mathcal{I}_t^c}^0 = \mathbf{0}$ .
  - 5:   **for**  $s = 1, \dots, s_{\max}$  **do**
  - 6:     Update  $\mathbf{u}_{\mathcal{I}_t}^s$  using PG ( $\lambda > 0$ ) or CGD ( $\lambda = 0$ ) rules.
  - 7:     Break if the stopping conditions are achieved.
  - 8:   **end for**.
  - 9:   Set  $\mathbf{x}_{\mathcal{I}_t}^t = \mathbf{u}_{\mathcal{I}_t}^k$ ,  $\mathbf{x}_{\mathcal{I}_t^c}^t = \mathbf{0}$  and  $\boldsymbol{\xi}^t = \mathbf{b} - \mathbf{A}_{\mathcal{I}_t} \mathbf{x}_{\mathcal{I}_t}^t$ . Let  $t = t + 1$ .
  - 10: **end while**
- 

When  $\lambda = 0$  and  $\varrho = 1$ , MPL in Algorithm 1 is reduced to the orthogonal matching pursuit (OMP) [40], [41]. MPL is also related to stagewise OMP (StOMP) [42] and stagewise weak gradient pursuits (SWCGP for short) [43], in the sense that all of them add a set of new atoms per iteration. However, in SWCGP and StOMP, the number of atoms added per iteration changes due to complex thresholding strategies [42], [43]. For example, in StOMP, the knowledge of noise is required to determine the number of new atoms. This knowledge, however, is not available for general problems [43]. To address this, SWCGP adopts a simpler thresholding strategy that is independent of the noise [43]. However, in SWCGP, only one iteration is conducted (namely  $s = 1$ ) in the master problem optimization. As a result, the master problem may not be sufficiently optimized, and many non-support atoms might be included accordingly, leading to degraded performance. In contrast, MPL takes more iterations in the master problem optimization before the following stopping condition is achieved:

$$\frac{f(\mathbf{u}^{s-1}) - f(\mathbf{u}^s)}{f(\mathbf{u}^0) - f(\mathbf{u}^s)} \leq \varepsilon_{in}, \quad (8)$$

where  $\varepsilon_{in}$  denotes a small tolerance.

### B. Subspace Exploratory Matching for MPL

The convergence of MPL has been studied in Part I [1]. However, the performance of MPL might be affected by the value of  $\varrho$ . To explain this, we first present a bound regarding the progress of objective value per outer loop.

**Lemma 1.** Let  $f(\mathbf{x}) = \|\mathbf{x}\|_1 + \frac{1}{2} \|\boldsymbol{\xi}\|^2$ ,  $\mathbf{g} = \mathbf{A}^\top \boldsymbol{\xi}^{t-1}$  and  $\mathbf{u}^1$  be the starting point regarding the inner loop. Assume  $|g_i| > \lambda$  for  $\forall i \in \mathcal{J}_{t+1}$ , where  $\mathcal{J}_{t+1}$  is obtained by Step 3 of Algorithm 1, with proper line search in PG, we have:

$$f(\mathbf{x}^t) - f(\mathbf{u}^1) \geq \frac{1}{2L} \sum_{i \in \mathcal{J}_{t+1}} (|g_i| - \lambda)^2,$$

where  $1/L$  is the step size obtained by the line search in PG.

According to Lemma 1, choosing  $\varrho$  atoms with the largest  $|g_i|$  can only guarantee the best improvement in objective values after one iteration (e.g.  $s = 1$ ) of the inner loop. However, these  $\varrho$  atoms cannot guarantee the best objective value improvement when more inner iterations (e.g. when  $s > 1$ ) are used. In other words, the worst-case analysis in Step 3 might be suboptimal when  $s > 1$ . When  $\varrho$  is relatively large in particular, some non-support atoms that are with large values of  $|g_i|$  might be mistakenly added into  $\mathcal{J}_t$ . To address this, we propose to first include more than  $\varrho$  (e.g.  $\omega\varrho$ , where  $\omega > 1$ ) new atoms with the largest  $|g_i|$ , and then solve the master problem in (7) with all of the selected atoms. Finally, we choose  $\varrho$  new atoms that decrease the objective value the most as the most-active atoms. This scheme, which is referred to as subspace exploratory matching, is summarized in Algorithm 2. To improve the efficiency, we adopt a warm-start strategy (see Step 3), and use equation (8) as the stopping condition in the master problem optimization.

---

**Algorithm 2** Subspace Exploratory Matching

---

- 1: Given a dictionary  $\mathbf{A}$ ,  $\mathcal{I}_{t-1}$ ,  $\boldsymbol{\alpha}^t$ ,  $\varepsilon_{in}$  and  $\omega (\omega \geq 1)$ .
  - 2: Calculate  $\mathbf{g} = \mathbf{A}^\top \boldsymbol{\alpha}^t$ ; choose the  $\omega\varrho$  largest  $|g_j|$  and record the indices in  $\mathcal{J}_\omega$ ; let  $\mathcal{I}_\omega = \mathcal{I}_{t-1} \cup \mathcal{J}_\omega$ .
  - 3: Initialize  $\mathbf{u}_{\mathcal{I}_\omega}^0 = \mathbf{x}_{\mathcal{I}_\omega}^{t-1}$  and  $\mathbf{u}_{\mathcal{I}_\omega^c}^0 = \mathbf{0}$ .
  - 4: **for**  $s = 1, \dots, s_{\max}$  **do**
  - 5:   Update  $\mathbf{u}_{\mathcal{I}_\omega}^s$  using PG ( $\lambda > 0$ ) or CGD ( $\lambda = 0$ ) rules.
  - 6:   Quit if the stopping conditions are achieved.
  - 7: **end for**.
  - 8: Sort the  $\omega\varrho$  atoms in  $\mathcal{J}_\omega$  in descending order by  $|u_i|$ ; return the first  $\varrho$  atoms and record the indices in  $\mathcal{J}_t$ .
  - 9: Let  $\mathcal{I}_t = \mathcal{I}_{t-1} \cup \mathcal{J}_t$ . Set  $\mathbf{x}_{\mathcal{I}_t}^t = \mathbf{u}_{\mathcal{I}_t}^s$  and  $\mathbf{x}_{\mathcal{I}_t^c}^t = \mathbf{0}$ .
- 

For convenience, hereafter we refer to Algorithm 1 with the subspace search as SMPL. In general, since the  $\varrho$  atoms chosen in SMPL achieve better improvement in objective value than MPL, both convergence speed and sparse recovery performance can be boosted, which can be observed in Fig. 1 in Section IV-B.

The proposed subspace search is related to the atom selection strategies used in CoSaMP [44], SP [45] and OMPR [46]. For example, to find  $k$  true supports, CoSaMP and SP choose  $2k$  and  $k$  additional atoms respectively into the active atom set. After that, a pruning step is performed such that only  $k$  atoms are kept in the active atom set. In contrast, there is no atom replacement or deletion in (S)MPL w.r.t. the outer iterations. Consequently, SMPL is guaranteed to monotonically decrease the objective values as in MPL [1]. Lastly, the subspace search of CoSaMP, SP and OMPR relies on the estimation of  $k$ , which is not required in SMPL.



### C. Stopping Conditions

Given a properly selected  $\lambda$ , a natural stopping condition for (S)MPL is

$$\|\alpha^\top \mathbf{A}\|_\infty \leq \lambda. \quad (9)$$

However, in practice, we may choose a small  $\lambda$  in order to reduce the solution bias of LASSO directly. When  $\lambda$  is very small, (S)MPL stops when  $\|\alpha\| \ll \|\mathbf{e}\|$  (here  $\mathbf{e}$  denotes the ground-truth noise), and it is possible that the over-fitting problem will happen. To prevent from the over-fitting problem, we stop (S)MPL early if the following stopping conditions are achieved:

$$\|\alpha^\top \mathbf{A}\|_\infty \leq r_\infty \quad \text{or} \quad \|\alpha\| \leq r_2, \quad (10)$$

where  $r_\infty$  and  $r_2$  are pre-determined parameters. We can also stop (S)MPL if

$$\frac{\delta^t}{|\varrho f(\mathbf{x}^0)|} \leq \varepsilon, \quad (11)$$

where  $\delta^t$  is the function value difference between the  $(t-1)^{\text{th}}$  and  $t^{\text{th}}$  iteration,  $\varepsilon$  is a small tolerance and  $f(\mathbf{x}^0)$  denotes the initial objective value.

Without early stopping, (S)MPL will achieve the LASSO solution, which may be biased (when  $\lambda$  is large) or over-fitted (when  $\lambda$  is small). For  $\lambda = 0$  and  $\varrho = 1$  in particular, (S)MPL will get the results of OMP [40], [41].

### D. Implementation Concerns

Several implementation techniques can be adopted to improve the efficiency of (S)MPL. Note that the master problem optimization in (S)MPL is w.r.t. a small set of atoms only. Let  $\mathcal{I}$  be the index set of selected atoms. We only need to calculate small scale matrix-vector products  $\mathbf{A}_{\mathcal{I}}\mathbf{x}_{\mathcal{I}}$  and  $\mathbf{A}_{\mathcal{I}}^\top \xi$ . For convenience, we refer to them as the partial matrix-vector product (PMVP). Correspondingly, we refer to  $\mathbf{A}\mathbf{x}$  and  $\mathbf{A}^\top \xi$  as the full matrix-vector product (FMVP).

Firstly, since  $|\mathcal{I}| \ll m$ , computing the PMVP (e.g.  $\mathbf{A}_{\mathcal{I}}\mathbf{x}_{\mathcal{I}}$  and  $\mathbf{A}_{\mathcal{I}}^\top \xi$ ) is much cheaper than FMVP (e.g.  $\mathbf{A}\mathbf{x}$  and  $\mathbf{A}^\top \xi$ ). To fully exploit this advantage, we store  $\mathbf{A}$  atom by atom in the main memory so that we can easily retrieve any atoms indexed by  $\mathcal{I}$  using C++ pointers.

Secondly, when dealing with big dictionaries, the cache-to-memory efficiency is important. For example, the calculations of PMVPs (e.g.  $\mathbf{A}_{\mathcal{I}}\mathbf{x}_{\mathcal{I}}$  and  $\mathbf{A}_{\mathcal{I}}^\top \xi$ ) may not be cache-to-memory efficient, since the active atoms in general are very far away from each other in the main memory. To address this, we explicitly store  $\mathbf{A}_{\mathcal{I}}$  and  $\mathbf{A}_{\mathcal{I}}^\top$  in the main memory. Accordingly, we can compute PMVPs very efficiently.

Thirdly, several iterations regarding the master problem optimization are sufficient, which significantly reduce the number of PMVPs. Moreover, once updating  $\mathcal{I}_t$ , we set  $\mathbf{x}_{\mathcal{I}_t}^t = \mathbf{u}_{\mathcal{I}_t}^s$  for the purpose of warm-start (see Step 9 in Algorithm 2). In this way, we can significantly improve the efficiency of the master problem optimization.<sup>2</sup>

<sup>2</sup>For fair comparison, we employ the above techniques to implement the  $\ell_1$ -norm methods whenever the intermediate variables are sparse: Let  $\mathcal{I}$  denote the supports of an intermediate  $\mathbf{x}$ , we replace  $\mathbf{A}\mathbf{x}$  with  $\mathbf{A}_{\mathcal{I}}\mathbf{x}_{\mathcal{I}}$ , which will improve the efficiency considerably.

### III. BATCH MODE MPL

In the batch SR problem, suppose there are  $p$  signals to be sparsely represented at the same time. Existing  $\ell_1$ -norm methods, such as PG [21] and FISTA [22], take  $O(mn)$  cost per iteration. Suppose they stop after  $S$  iterations, the total cost for recovering  $p$  signals is  $O(Spmn)$ . On the contrary, suppose (S)MPL stops after  $T$  iterations, it will reduce the cost to  $O(Tpmn)$ , where  $T \ll S$ .

Nevertheless, the complexity of MPL and SMPL is still dependent on  $n$ , making them expensive to tackle large-scale problems that are with large  $n$ . Essentially, this computational burden is brought by the calculation of  $\mathbf{A}^\top \xi$  (which takes  $O(mn)$  cost) in the worst-case analysis. Therefore, how to reduce the cost of  $\mathbf{A}^\top \xi$  is critical for improving the efficiency.

According to the studies in [17], [42], if the discrete Fourier transform basis or wavelet basis are sampled to form the dictionary  $\mathbf{A}$ , the computational complexity of  $\mathbf{A}^\top \xi$  can be reduced to  $O(m \log(m))$  with the help of the fast Fourier transform (FFT). However, this technique cannot be applied to general dictionaries.

To tackle many signals under general dictionaries, we propose below the **batch-mode MPL** (BMPL for short), in which the computational cost can be greatly reduced. Actually, we have  $\mathbf{A}^\top \xi = \mathbf{A}^\top (\mathbf{b} - \mathbf{A}_{\mathcal{I}}\mathbf{x}_{\mathcal{I}}) = \mathbf{A}^\top \mathbf{b} - [\mathbf{A}^\top \mathbf{A}_{\mathcal{I}}]\mathbf{x}_{\mathcal{I}}$ . Let  $\beta = \mathbf{A}^\top \mathbf{b}$  and  $\mathbf{Q} = \mathbf{A}^\top \mathbf{A}$ . If we pre-compute  $\mathbf{Q}$  and  $\beta$ , and store them in the main memory, we can then calculate  $\mathbf{A}^\top \xi$  according to

$$\mathbf{A}^\top \xi = \beta - \mathbf{Q}_{\mathcal{I}}\mathbf{x}_{\mathcal{I}}. \quad (12)$$

As a result, the computation cost of computing  $\mathbf{A}^\top \xi$  is reduced to  $O(m|\mathcal{I}|)$ , where  $|\mathcal{I}| \ll n$ . Since  $|\mathcal{I}| \approx k$ , the overall cost for  $p$  signals becomes  $O(Tpmk)$ .

**Remark 1.** To apply (12), we need to compute the matrix  $\mathbf{Q} \in \mathbb{R}^{m \times m}$  with  $O(nm^2)$  cost, which is not efficient regarding a single signal. However, since  $\mathbf{Q}$  can be calculated off-line, this cost is negligible when dealing with many signals.

Since BMPL adds  $\varrho$  atoms per iteration, it requires considerably fewer times of  $\mathbf{A}^\top \xi$  than the batch mode OMP (BOMP for short) [24]. Specifically, BOMP takes  $O(pmk^2)$  cost for  $p$  signals; while BMPL takes  $O(Tpmk)$  complexity, where  $T \ll k$ .

For existing  $\ell_1$ -norm methods, even though the intermediate variables are sparse, it is not easy for them to conduct the batch mode optimization, since the support set  $\mathcal{I}$  of intermediate variables might change frequently during the optimization. As a result, frequent retrievals of  $\mathbf{Q}_{\mathcal{I}}$  are very computationally expensive.

The batch scheme is not applicable to a dictionary with a very large number of atoms, because of the  $O(m^2)$  space complexity to store  $\mathbf{Q}$ . Nevertheless, BMPL can be applied to many large-scale tasks. For example, it can efficiently deal with dictionaries of  $O(2^{15})$  atoms on a 24GB memory machine, which is sufficient for many real-world applications, such as face recognition [7] and dictionary learning [10].

#### IV. NUMERICAL EXPERIMENTS

In this section, we compare the performance of (S)MPL with the following baseline methods:<sup>3</sup>

- Four state-of-the-art  $\ell_1$ -solvers: Shotgun<sup>4</sup> which uses the parallel coordinate descent in C++ [47]. FISTA<sup>5</sup> which uses the accelerated proximal gradient method with continuation technique [17], [25]; PGH which uses the homotopy method to improve the convergence speed [18], [19]; S-L1<sup>6</sup> which adopts a screening test to predict the zero entries to improve the decoding efficiency [48].
- Several related greedy methods, such as ROMP [49]<sup>7</sup>, StOMP [42]<sup>8</sup> and SWCGP [43] are used for the comparison. In addition, four well-known greedy algorithms, i.e. orthogonal matching pursuit (OMP) [40], [41], accelerated iterative hard thresholding (AIHT) [50], [51], [52]<sup>9</sup>, subspace pursuit (SP) [45]<sup>10</sup> and orthogonal matching pursuit with replacement (OMPR) [46], are also included as baseline methods.

In the experiments, Shotgun is conducted in parallel on an Intel(R) Core(TM) i7 CPU (8 cores) PC with 64-bit Linux OS; while the other methods are conducted on a 64-bit Windows operating system (OS) with the same computer configuration. For fair comparison, all methods, except S-L1, ROMP and StOMP, are written in C++ running with **single core**. We run S-L1, which is written in Matlab, in parallel on an eight-core machine.

##### A. Experimental Settings and Performance Metrics

Following [18], [17], we set  $\lambda = 0.005\|\mathbf{A}^\top \mathbf{b}\|_\infty$  for  $\ell_1$ -norm methods. Unless noted otherwise, we apply **de-biasing technique** to reduce the solution bias of  $\ell_1$ -norm methods [17], [25]. For (S)MPL, we apply the early stopping to avoid the over-fitting problem with stopping condition

$$|\delta^t|/(\varrho\|\mathbf{b}\|^2) \leq 1.0 \times 10^{-5}, \quad (13)$$

where  $\delta^t$  denotes the objective difference between the  $t$ th and  $(t+1)$ th iterations. We set the subspace search length  $\omega = 3$  for SMPL. For many greedy methods, such as AIHT, SP and OMPR, we need to specify  $\hat{k}$ . In the simulation, since we know the ground-truth  $k$ , we set  $\hat{k} = 1.2k$ . For OMPR,  $\eta$  is set to 0.7. Lastly, we keep default settings of other parameters for the baseline methods.

Following [45], [18], [19], we study compressive sensing problems over *Gaussian* design matrices. We study two types of sparse signals, e.g. *Bernoulli* sparse vector (denoted by  $\mathbf{s}_z$  with each nonzero entry being either 1 or -1) and *Gaussian* sparse signal (denoted by  $\mathbf{s}_g$  with each nonzero entry being sampled from *Gaussian* distribution  $\mathcal{N}(0, 1)$ ). The observation

$\mathbf{b}$  is produced by  $\mathbf{b} = \mathbf{A}\mathbf{x} + \mathbf{e}$ , where  $\mathbf{e}$  denotes the additive noise uniformly sampled from  $[-0.01, 0.01]$ .

To evaluate the sparse recovery performance of a method, we adopt the *root-mean-square error* (RMSE) as the comparison metric,

$$\text{RMSE} = \sqrt{\sum_{i=1}^m (x_i^* - x_i)^2 / m},$$

where  $\mathbf{x}^*$  denotes the recovered signal. Here, a sparse signal is successfully recovered if  $\text{RMSE} \leq 1\text{E}-3$ . For a complete comparison, we record the *empirical probability of successful reconstruction* (EPSR) over  $M$  independent experiments [45].

##### B. Comparison with PGH, FISTA and Active-set Method

We compare (S)MPL with PGH, FISTA and Active-set methods on recovering a 140-sparse *Bernoulli* sparse signal and a 140-sparse *Gaussian* sparse signal over a *Gaussian* dictionary  $\mathbf{A} \in \mathbb{R}^{2^{10} \times 2^{13}}$ . To study the effect of  $\varrho$ , given a basic  $\varrho$ , we study  $2\varrho$  and  $4\varrho$ . We study two  $\lambda$ 's, namely  $\lambda_1 = 0.005\|\mathbf{A}^\top \mathbf{b}\|_\infty$  and  $\lambda_2 = 0.00005\|\mathbf{A}^\top \mathbf{b}\|_\infty$ . In Fig. 1, we report the objective values of the comparison methods w.r.t. iterations. In Table I and Table II, we record the following metrics: The number of full matrix-vector products (#FMVPs); The number of partial matrix-vector products (#PMVPs); The number of nonzeros (*Sparsity*) in solutions; The decoding time (*Time*) for each signal; The speedup (*#speedup*) of the fastest method over others.

Based on the results, we draw the following conclusions.

- From Fig. 1, (S)MPL with different  $\varrho$ 's converge much faster than baseline methods. In particular, **SMPL( $2\varrho$ ) is about 20 times faster** than others on the *Gaussian* sparse signal. FISTA converges well when  $\lambda = 0.005\|\mathbf{A}^\top \mathbf{b}\|_\infty$ . In particular, the objective value decreases very quickly at the beginning. However, it converges very slowly when  $\lambda = 0.00005\|\mathbf{A}^\top \mathbf{b}\|_\infty$ . In fact, generally speaking, the convergence rate of FISTA is only sub-linear, e.g.  $O(1/k^2)$  [22]. In contrast to FISTA, PGH solves a sequence of subproblems, and attain linear convergence rate if the subproblem is strongly convex [18], [19]. Overall, it performs much better than FISTA.
- Note that each FMVP takes  $O(mn)$  complexity. From Tables I and II, (S)MPL with different  $\varrho$ 's need far fewer FMVPs than other methods, which explains the significant speedup of (S)MPL over other methods. Therefore, (S)MPL are more suitable for big dictionaries.
- From Tables I and II, in general, (S)MPL also need much fewer number of PMVPs than others. Moreover, the scale of PMVPs in (S)MPL is much smaller than in PGH and FISTA. For example, when  $\lambda = 0.00005\|\mathbf{A}^\top \mathbf{b}\|_\infty$ , the sparsity of the PGH solution is 1015, which is much larger than that of (S)MPL. In other words, the master problem optimization in PGH is more expensive.
- If  $\varrho$  is too large, MPL may take more computation time. For example, from Table I, MPL with  $2\varrho$  indeed needs less time than MPL with  $4\varrho$ . The reason is that, if  $\varrho$  is large, some non-support atoms might be mistakenly

<sup>3</sup>The C++ source codes of MPL and the compared methods are available at: <http://www.tanmingkui.com/mpl.html>.

<sup>4</sup><https://www.select.cs.cmu.edu/projects>.

<sup>5</sup><https://www.eecs.berkeley.edu/~yang/software/11benchmark/index.html>.

<sup>6</sup><http://www.princeton.edu/~zxliang/home/index.html>.

<sup>7</sup><https://www-personal.umich.edu/~romanv/software/romp.m>.

<sup>8</sup><https://sparselab.stanford.edu/>.

<sup>9</sup><https://www.personal.soton.ac.uk/tb1m08/publications.html>.

<sup>10</sup><https://sites.google.com/site/igorcarron2/cscodes>.

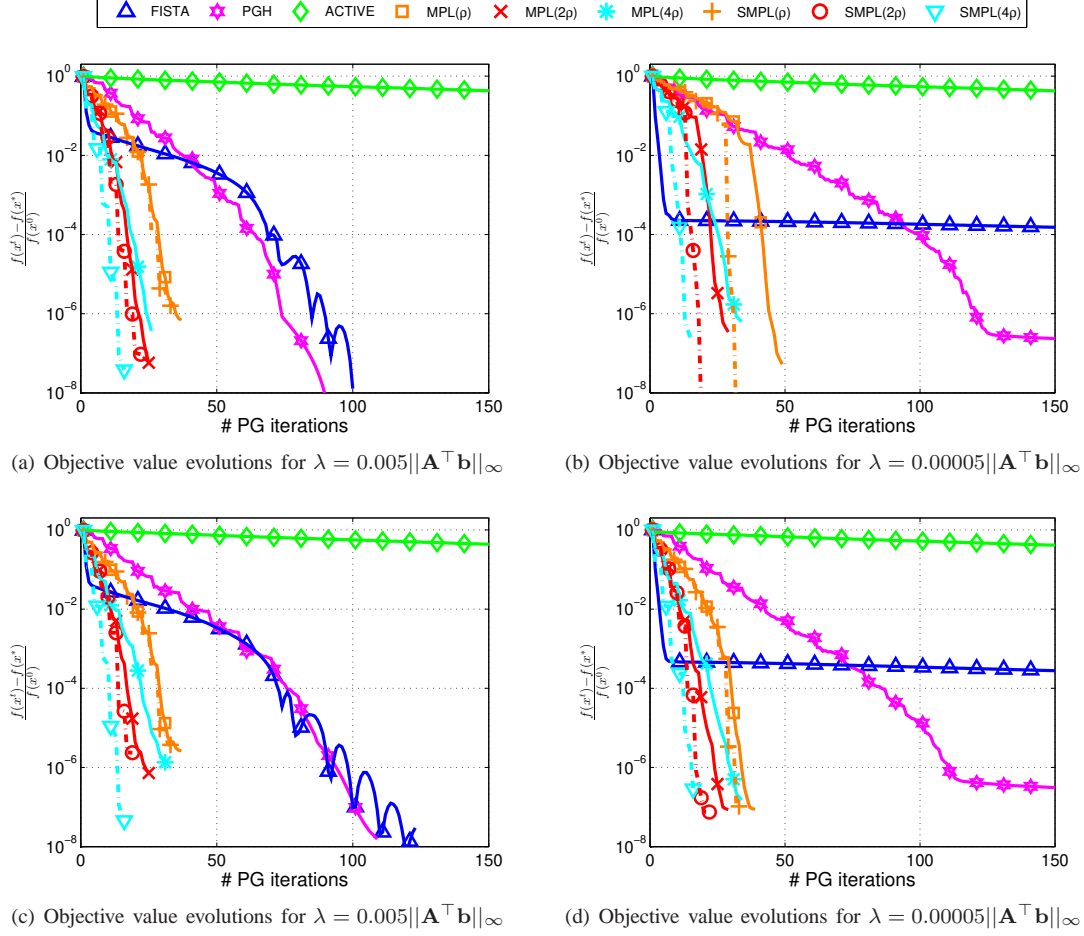


Fig. 1. Convergence of the comparison methods on *Bernoulli* sparse vectors (in Fig. 1(a) and 1(b)) and *Gaussian* sparse vectors (in Fig. 1(c) and 1(d)). For (S)MPL and the Active-set method, we record  $f(\mathbf{x}^t)$  per PG iteration. We only record results within 150 iterations for all methods.

TABLE I  
COMPARISON AMONG MPL, FISTA, PGH AND ACTIVE-SET METHODS ON *Bernoulli* SPARSE SIGNAL, WHERE *Time* RECORDS THE DECODING TIME (IN SECONDS).

$\lambda$		Active-set	FISTA	PGH	MPL( $\rho$ )	SMPL( $\rho$ )	MPL( $2\rho$ )	SMPL( $2\rho$ )	MPL( $4\rho$ )	SMPL( $4\rho$ )
$0.005\ \mathbf{A}^\top \mathbf{b}\ _\infty$	<i>Sparsity</i>	160	595	253	159	168	216	166	188	178
	#FMVP	160	120	177	11	11	7	5	4	3
	#PMVP	2591	344	344	228	450	183	238	134	171
	<i>Time</i>	1.36	6.07	1.22	0.11	0.14	0.09	0.08	<b>0.06</b>	<b>0.07</b>
	#speedup	21.9	97.9	19.6	1.8	2.3	1.5	1.3	1	1.3
$0.00005\ \mathbf{A}^\top \mathbf{b}\ _\infty$	<i>Sparsity</i>	161	1015	1015	189	144	244	195	328	197
	#FMVP	160	1000	160	13	10	8	6	5	3
	#PMVP	2647	3021	473	279	418	202	281	175	170
	<i>Time</i>	1.47	98.37	2.78	0.12	0.14	0.09	0.09	<b>0.08</b>	<b>0.08</b>
	#speedup	18.8	1261.2	35.6	1.6	1.8	1.2	1.2	1.0	1.0

TABLE II  
COMPARISON AMONG MPL, FISTA, PGH AND ACTIVE-SET METHODS ON *Gaussian* SPARSE SIGNAL, WHERE *Time* RECORDS THE DECODING TIME (IN SECONDS).

$\lambda$		Active-set	FISTA	PGH	MPL( $\rho$ )	SMPL( $\rho$ )	MPL( $2\rho$ )	SMPL( $2\rho$ )	MPL( $4\rho$ )	SMPL( $4\rho$ )
$0.005\ \mathbf{A}^\top \mathbf{b}\ _\infty$	<i>Sparsity</i>	160	313	221	154	154	196	168	303	256
	#FMVP	160	79	92	10	10	6	5	5	4
	#PMVP	2578	255	280	195	414	146	235	152	208
	<i>Time</i>	1.40	4.46	0.92	0.09	0.14	<b>0.06</b>	0.09	<b>0.06</b>	0.09
	#speedup	22.3	70.8	14.6	1.5	2.2	1.0	1.5	1.0	1.5
$0.00005\ \mathbf{A}^\top \mathbf{b}\ _\infty$	<i>Sparsity</i>	160	1015	1015	166	154	222	194	391	280
	#FMVP	201	1000	144	11	10	7	6	6	4
	#PMVP	3271	3023	611	238	415	183	282	202	239
	<i>Time</i>	1.92	92.41	2.28	0.12	0.12	<b>0.09</b>	<b>0.09</b>	<b>0.09</b>	0.11
	#speedup	20.5	983.1	24.2	1.3	1.3	1.0	1.0	1.0	1.2

included. From Fig. 1, SMPL in general converges faster than MPL with a large  $\rho$ , which demonstrates the effectiveness of the *subspace exploratory search*.

- From Tables I and II, the recovered signals are not exactly 140-sparse. This is because the observation  $\mathbf{b}$  has been disturbed by the noises  $\mathbf{e}$ .

TABLE III  
AVERAGED SPARSITY OF SOLUTIONS OBTAINED BY VARIOUS METHODS  
WITH  $k = 140, 160, 180$ , RESPECTIVELY.

$k$	ROMP	StOMP	SWCGP	MPL	SMPL
140	506	260	230	167	154
160	584	309	359	182	168
180	651	374	432	196	210

### C. Influences of $\omega$ on SMPL

In this experiment, we conduct a sensitivity study on  $\omega$  for SMPL. We fix  $\lambda = 0.00005\|\mathbf{A}^\top \mathbf{b}\|_\infty$  and vary  $\omega \in \{1, 2, 3, 4, 5\}$ . Note that SMPL is reduced to MPL when  $\omega = 1$ . For each  $k \in \{270, 280, \dots, 360\}$ , we conduct  $M = 100$  independent experiments, and record the EPSR values and averaged decoding time in Fig. 2(a) and Fig. 2(b), respectively.

From Fig. 2(a), SMPL with larger  $\omega$ 's tends to have better recovery performance in terms of EPSR. However, when  $\omega > 3$ , the improvement becomes less significant. The reason is that, if  $\omega$  is large enough (e.g.  $\omega = 3$ ), the  $\omega\rho$  atoms with largest  $|g_i|$  already include most of the potential active atoms, thus the increasing  $\omega$  will not significantly improve the performance. From Fig. 2(b), MPL (e.g. SMPL with  $\omega = 1$ ) shows the worst decoding efficiency. The reason is that, without the subspace search, some non-support atoms might be mistakenly included, and MPL needs more iterations to converge.

### D. Comparisons with ROMP, StOMP, and SWCGP

We compare (S)MPL with ROMP, StOMP, and SWCGP on *Gaussian* sparse signals, where  $\mathbf{A} \in \mathbb{R}^{2^{10} \times 2^{13}}$ . We use the default parameter settings for StOMP and SWCGP. We conduct  $M = 100$  independent experiments for each  $k \in \{80, 100, \dots, 360\}$ , and record the EPSR value and the averaged decoding time in Fig. 3(a) and Fig. 3(b), respectively. We also record the sparsity of solutions for  $k \in \{140, 160, 180\}$  in Table III.

From Fig. 3(a) and Fig. 3(b), (S)MPL outperforms the two baselines in terms of sparse recovery performance and decoding efficiency. StOMP cannot successfully recover all the sparse signals when  $k > 240$ . From Table III, StOMP and SWCGP include more atoms than (S)MPL, which indicates that many non-support atoms have been included. This problem becomes more severe for SWCGP, since its master problem is not sufficiently optimized. As a result, it cannot recover all the  $k$ -sparse signals when  $k > 180$ , as shown in Fig. 3(a). Lastly, ROMP shows much worse sparse recovery performance than other methods, which is consistent with the conclusions in [43].

### E. Comparisons with Other Baselines

In this experiment, we compare the performance of (S)MPL with other baseline methods on a median-scale problem  $\mathbf{A} \in \mathbb{R}^{2^{10} \times 2^{13}}$ , where Shotgun and S-L1 work in **parallel**. For each  $k$ , we run  $M = 100$  independent trials. For (S)MPL, we apply early stopping to avoid the over-fitting problem.

In OMPR, it is necessary to calculate  $\mathbf{z} = \mathbf{x} + \eta \mathbf{A}^\top (\mathbf{b} - \mathbf{A}\mathbf{x})$ , where  $\eta$  is a learning rate of OMPR [46]. The setting of  $\eta$  is crucial for the performance [46]. In [46], a feasible range for  $\eta$  is provided if  $\mathbf{A}$  satisfies the RIP condition. Unfortunately, if  $\mathbf{A}$  is not well scaled, the scale of  $\mathbf{A}^\top (\mathbf{b} - \mathbf{A}\mathbf{x})$  may vary a lot and the setting of  $\eta$  will be difficult.<sup>11</sup> To address this issue, we propose a variant of OMPR in which  $\eta$  is adaptively adjusted by applying the CGD rule. *To distinguish this variant from OMPR, we refer it to as the OMPRA.*

The EPSR value and recovery time for the *Gaussian* sparse signals of each method are presented in Fig. 4. From this figure, SMPL and OMP show much better recovery performance than other methods on the *Gaussian* sparse signals in terms of EPSR. In general, SMPL shows better recovery performance than MPL in terms of EPSR. OMPR [46] shows worse recovery performance than other greedy methods. From the experiments, OMPRA that uses an adaptive learning rate improves OMPR greatly. However, OMPRA is still worse than (S)MPL.

From Fig. 4(b), MP algorithms are much faster than the  $\ell_1$ -norm methods, such as Shotgun (a well-designed parallel  $\ell_1$ -method) and PGH. Ultimately, PGH shows better efficiency than Shotgun and S-L1, but is much worse than (S)MPL.

### F. Scalability Comparisons on Big Dictionaries

In the final experiment, we compare the scalability of (S)MPL with several baselines on a Big Dictionary  $\mathbf{A} \in \mathbb{R}^{2^{12} \times 2^{20}}$  with two experiments.<sup>12</sup> Here, only *Gaussian* sparse signals are studied.

In the first experiment, we generate  $k$ -sparse signals with  $k \in \{300, 400, \dots, 800\}$ , and compare (S)MPL with FISTA, PGH, SP and AIHT. We set  $\hat{k} = 1.2k$  for SP and AIHT. We set  $\lambda = 0.005\|\mathbf{A}^\top \mathbf{b}\|_\infty$  for LASSO related algorithms, and set the maximum iterations of FISTA and PGH to 150. We report the RMSE and recovery time in Fig. 5(a) and Fig. 5(b), respectively. According to the reported results, the following conclusions can be drawn.

- From Fig. 5(a), (S)MPL shows better RMSE than other methods when  $500 < k \leq 600$ ; SMPL significantly improves MPL in terms of RMSE when  $650 < k < 700$ . In addition, SP and AIHT cannot recover the  $k$ -sparse signal if  $k > 600$  (the RMSE values are very large). Lastly, PGH and FISTA show worse recovery performance than other methods in terms of RMSE, which coincides with the results in Tables I and II.
- From Fig. 5(b), it is evident that (S)MPL is much more efficient than other methods, in particular when  $k \geq 500$ .

<sup>11</sup>Interested readers can find more details of  $\eta$  in [46].

<sup>12</sup>In real-world applications, such as the face recognition task, we may have more than 1 million training images from many persons [53]. In SR based face recognition, the training images are formed as a big dictionary.



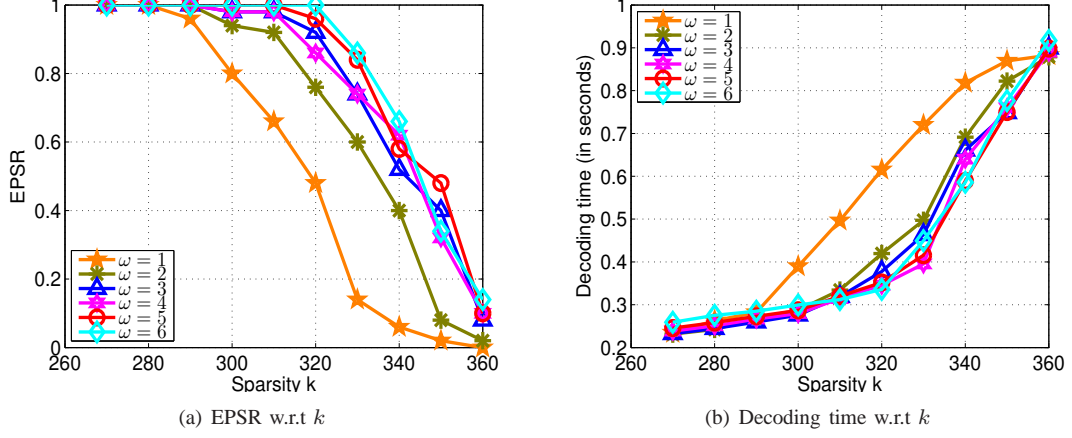


Fig. 2. Results of SMPL on Gaussian sparse signals with different  $\omega$ 's.

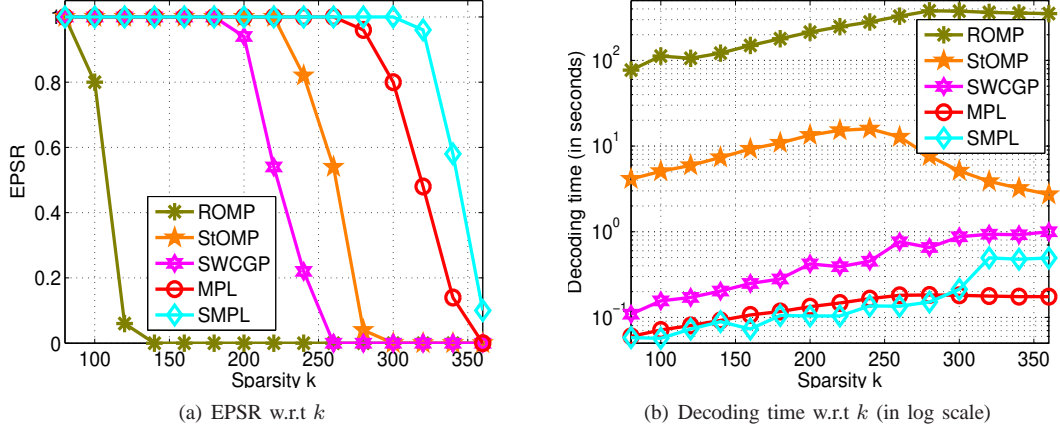


Fig. 3. Comparison among ROMP, StOMP, SWCGP, MPL and SMPL on Gaussian sparse signals, where the early stopping according to the condition (13) is applied to StOMP, SWCGP, MPL and SMPL.

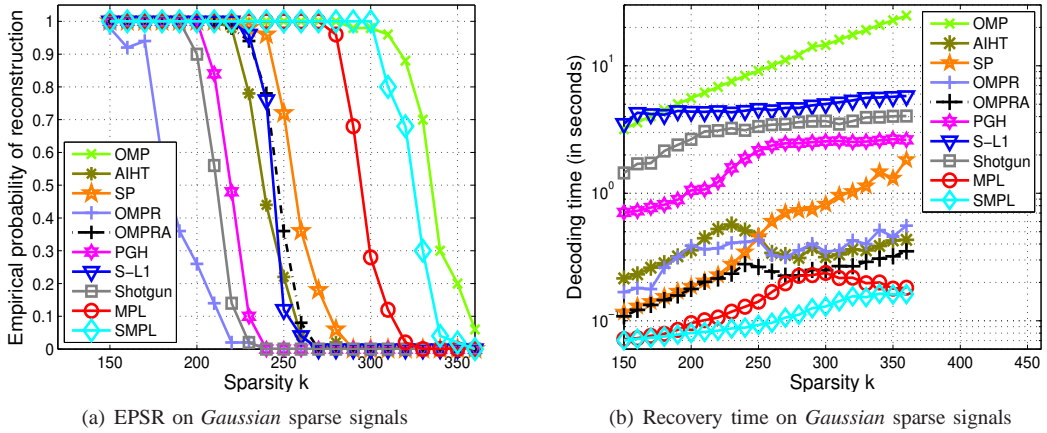


Fig. 4. SR results on  $\mathbf{A} \in \mathbb{R}^{2^{10} \times 2^{13}}$  of different methods. Here, the de-biasing technique is applied to  $\ell_1$ -norm methods, and the early stopping is applied to (S)MPL.



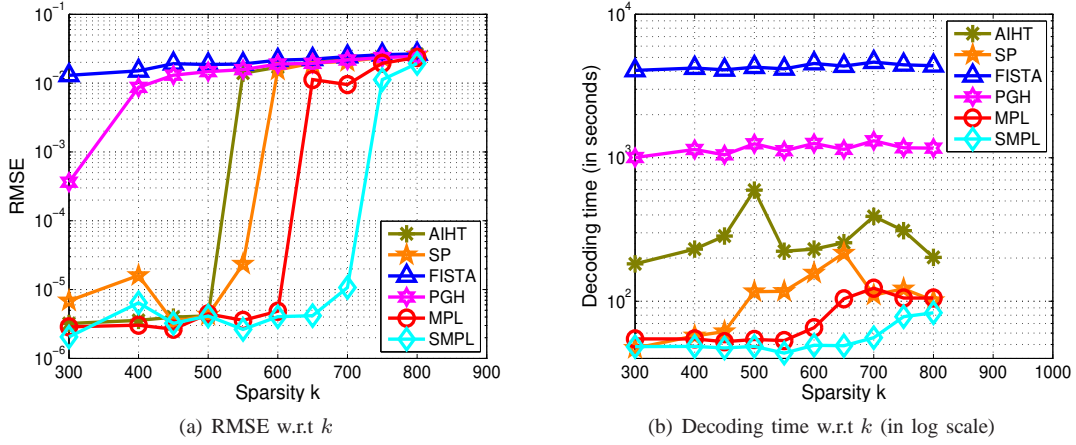


Fig. 5. SR results on Gaussian sparse signals under a *Big Dictionary*  $\mathbf{A} \in \mathbb{R}^{2^{12} \times 2^{20}}$ .

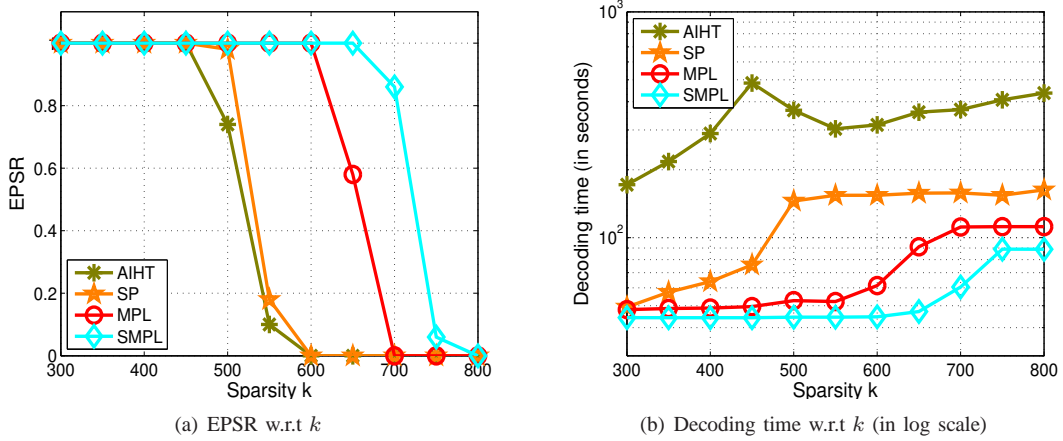


Fig. 6. SR performance comparison under a *Big Dictionary*  $\mathbf{A} \in \mathbb{R}^{2^{12} \times 2^{20}}$ .

SP has comparable efficiency with (S)MPL when  $k \leq 450$ , but becomes less efficient when  $k > 450$ . PGH and FISTA need thousands of seconds for all  $k$ 's; while MPL needs less than 100 seconds when  $k \leq 600$ . In particular, SMPL needs less than 50 seconds when  $k \leq 700$ .

- From Fig. 5(a), it is clear that PGH is better than FISTA in terms of RMSE. In general, PGH converges faster than FISTA, thus it achieves a better solution with the same number of iterations.

There are two reasons for the inefficiency of PGH and FISTA. Firstly, both of them require many iterations to converge, which means that they need to compute many times of  $\mathbf{A}^\top \boldsymbol{\xi}$  than (S)MPL. Secondly, when computing  $\mathbf{A}^\top \boldsymbol{\xi}$  for large dictionaries, the data exchange between the main memory and cache memory are very inefficient. In contrast, in (S)MPL, the master problem optimization is w.r.t. a small set of active atoms only, e.g.  $\mathbf{A}_{\mathcal{I}}$ . Apparently, the data exchange between the main memory and cache memory w.r.t.  $\mathbf{A}_{\mathcal{I}}$  is much more efficient.

To thoroughly compare the scalability of (S)MPL with SP and AIHT, in the second experiment, we run  $M = 100$  independent experiments for each  $k$ , where we exclude FISTA and PGH from the comparison. Here, we set  $\hat{k} = 1.5k$  for SP and AIHT. We record the EPSR value and averaged recovery

time in Fig. 6(a) and Fig. 6(b), respectively. From Fig. 6(a), (S)MPL shows much better recovery performance than SP and AIHT in terms of EPSR value. From Fig. 6(b), (S)MPL is also much more efficient than SP and AIHT.

## V. BATCH MPL AND APPLICATIONS TO MANY-FACE RECOGNITION

In this section, we first compare BMPL with BOMP on synthetic compressive sensing tasks, and then apply them to many-face recognition tasks.

### A. Comparison of BMPL and BOMP

BOMP is a batch mode implementation of OMP [24]. In the simulation, we generate a *Gaussian* random matrix  $\mathbf{A} \in \mathbb{R}^{2^{12} \times 2^{14}}$  and generate 200 *Gaussian* sparse signals for each sparsity  $k \in \{400, 450, 500, 550, 600\}$ . The vector of measurements  $\mathbf{b}$  is produced by  $\mathbf{b} = \mathbf{A}\mathbf{x} + \boldsymbol{\xi}$  with *Gaussian* noise sampled from  $\mathcal{N}(0, 0.05)$ . The total time (in seconds) spent by BMPL and BOMP in decoding 200 signals and the *averaged root-mean-square error (ARMSE)* are reported in Table IV. From Table IV, BMPL is **about 7-16 times faster** than BOMP. Moreover, BMPL gains better or comparable **ARMSE** to BOMP for all  $k$ .

TABLE IV  
EFFICIENCY COMPARISON BETWEEN BMPL AND BOMP (IN SECONDS).  
THE TIME CONSUMED FOR COMPUTING  $\mathbf{A}^\top \mathbf{A}$  IS 46.27 SECONDS

	$k$	400	450	500	550	600
BOMP	Time	434.27	546.70	680.96	835.72	1014.93
	ARMSE	7.11E-03	7.69E-03	7.92E-03	8.59E-03	8.94E-03
BMPL	Time	55.06	55.79	56.79	59.51	59.91
	ARMSE	3.88E-03	4.31E-03	4.36E-03	4.70E-03	4.93E-03
	#speedup	<b>7.89</b>	<b>9.80</b>	<b>11.99</b>	<b>14.04</b>	<b>16.94</b>

Note that it takes only 46.27 seconds to calculate  $\mathbf{A}^\top \mathbf{A}$ . In other words, the consumed time per signal is only 0.23 seconds. If there are 200,000 signals, then the computational time per signal will be  $2.3 \times 10^{-4}$  seconds, which is negligible.

### B. Many-face Recognition by BMPL

We apply BMPL for many-face recognition tasks by solving problem (3). We adopt L2 [33], L2-L2 [34] and BOMP [24] as the baseline methods. Besides, the PGH method is adopted for the comparison, since it has shown better efficiency than other  $\ell_1$ -norm methods [18], [19]. We follow the experimental settings in [7] for the comparison, which is negligible. We set  $\rho = 10$  for BMPL and  $k = 200$  for BOMP for all experiments. Furthermore, considering that there may be some images that cannot be sparse-represented by the training images, we constrain  $k \leq 600$ .

The *Extended YaleB* and *AR* databases are used for the comparison. The *Extended YaleB* database consists of 2,414 frontal face images of 38 subjects [33], [30]. They are captured under various lighting conditions and cropped and normalized to  $192 \times 168$  pixels. In our experiment, we take 62 images per person, resulting in 2,356 images in total. The *AR* database consists of over 2,600 frontal images of 100 individuals [54], [7], [30]. Each image is normalized to  $80 \times 60$  pixels. Computing  $\mathbf{A}^\top \mathbf{A}$  with all images of *Extended YaleB* and *AR* takes 5.74 seconds and 1.10 seconds, respectively. In other words, the time spent on  $\mathbf{A}^\top \mathbf{A}$  is negligible.

We consider two experimental settings: 1) *Many-face recognition with different number of pixels*; and 2) *Many-face recognition with different number of training samples*.

1) *Many-face Recognition with Different Number of Pixels*: In this experiment, we down-sample the images at a sampling rate  $\rho_d$ , where  $\rho_d$  is chosen from  $\{1, 1/2, 1/3, 1/4, 1/5, 1/6, 1/7\}$  for *YaleB* images, and  $\{1, 3/4, 2/3, 1/2, 1/3\}$  for *AR* images. Accordingly, the dimension of each new image vector will be  $\rho_d^2$  of the original image vector. Following [33], we randomly choose half of the images of each person as the training set, and the remaining images as the testing set. The prediction accuracies on the *YaleB* and *AR* images are shown in Table V. To measure the difference between results, the *Wilcoxon* test with 5% significance is conducted between BMPL and the winner of L2 and L2-L2, and 1 indicates the significant difference.

From Table V, on the *YaleB* database, BMPL shows significantly better accuracy than L2 and L2-L2 methods under  $\rho_d = 1/5, 1/6$  and  $1/7$ , and comparable or slightly better performance under other down-sampling rates. On the *AR*

TABLE VIII  
PREDICTION ACCURACY ON *YaleB* WITH DIFFERENT NUMBER OF TRAINING IMAGES

$\rho_t$	0.55	0.60	0.65	0.70	0.75	0.80
L2	0.6352	0.9350	0.9330	0.9684	0.9764	0.9815
L2-L2	0.9814	0.9814	0.9823	0.9827	0.9843	0.9872
BMPL	0.9848	0.9887	0.9887	0.9908	0.9911	0.9925
Wilcoxon	0	1	1	1	1	1

database, BMPL performs significantly better than L2 and L2-L2 methods under  $\rho_d = 1, 3/4$  and  $2/3$ . BMPL in particular shows much more stable performance than the L2 and L2-L2 methods. In particular, on the *AR* database, L2 only achieves **73.23%** prediction accuracy at a down-sampling rate  $\rho_d = 1/2$ , which may be caused by the unstable pseudo inverse on the ill-conditioned matrix [33]. As a regularized L2 method, L2-L2 method shows more stable performance than L2. However, it is still worse than BMPL.

We report the total time spent by various methods in Table VI. PGH, the state-of-the-art  $\ell_1$ -solver, needs several hours to predict all testing images on the *AR* database with  $\rho_d = 1$ , which is unbearable for many real-world applications. On the contrary, BMPL completes the prediction in 20 seconds only, which is 366 times faster than PGH. BMPL is also 3-10 times faster than BOMP. Lastly, BMPL achieves comparable efficiency to L2-L2 and L2.

A remaining question is: *does the sparsity help to improve recognition performance?* We list the average sparsity of BMPL, PGH, and BOMP in Table VII. Note that the solutions obtained by L2 and L2-L2 methods are not sparse. From Table V, BMPL, PGH, and BOMP show comparable or significantly better recognition rates than L2 and L2-L2 methods on the *YaleB* database. In addition, BMPL outperforms L2 and L2-L2 methods on *AR* database with enough pixels. Therefore, sparsity indeed **helps to improve** recognition rates.

2) *Face Recognition with Different Number of Training Samples*: Let  $\rho_t$  be the ratio of the number of training images over the total number of images. In this experiment, we vary  $\rho_t \in \{0.55, 0.60, 0.65, 0.7, 0.75, 0.8\}$  to change the number of training images. The prediction accuracy and prediction time w.r.t.  $\rho_t$  are shown in Tables VIII and IX, respectively.

In general, with more training images, the matrix  $\mathbf{A}^\top \mathbf{A}$  becomes more ill-conditioned. From Table VIII, BMPL performs significantly better than L2 and L2-L2 when  $\rho_t \geq 0.60$ . In other words, BMPL achieves more stable performance when  $\mathbf{A}^\top \mathbf{A}$  becomes more ill-conditioned. Finally, from Table IX, BMPL shows comparable efficiency to L2 and L2-L2 methods.

TABLE IX  
TOTAL TIME SPENT ON *YaleB* WITH DIFFERENT NUMBER OF TRAINING IMAGES (IN SECONDS)

$\rho_t$	0.55	0.60	0.65	0.70	0.75	0.80
L2	2.48	2.95	3.02	3.16	3.56	6.02
L2-L2	2.20	2.51	3.50	3.94	3.21	6.06
BMPL	10.65	6.11	5.71	4.93	4.23	2.85

## VI. CONCLUSIONS

In this paper, we have proposed a subspace search to further improve the performance of MPL, and a batch-mode MPL

TABLE V  
PREDICTION ACCURACY ON TWO FACE DATABASES

	Extended YaleB Database							AR Database				
$\rho_d$	1	1/2	1/3	1/4	1/5	1/6	1/7	1	3/4	2/3	1/2	1/3
L2	0.9876	0.9868	0.9831	0.9792	0.9371	0.9561	0.9621	0.9466	0.9301	0.9108	<b>0.7323</b>	0.9638
L2-L2	0.9898	0.9859	0.9827	0.9818	0.9783	0.9730	0.9723	0.9524	0.9504	0.9532	0.9574	0.9692
PGH	0.9897	0.9843	0.9826	0.9846	0.9815	0.9760	0.9658	0.9657	0.9650	0.9715	0.9679	0.9656
BOMP	0.9904	0.9897	0.9861	0.9844	0.9786	0.9799	0.9734	0.9742	0.9744	0.9738	0.9738	0.9619
BMPL	0.9911	0.9892	0.9873	0.9849	0.9817	0.9787	0.9761	0.9739	0.9757	0.9715	0.9723	0.9672
Wilcoxon	0	0	0	0	1	1	1	1	1	1	1	0

TABLE VI  
TOTAL TIME SPENT ON TWO FACE DATABASES (IN SECONDS), #SPEEDUP DENOTES THE TIMES OF SPEEDUP OF BMPL OVER PGH

	Extended YaleB Database							AR Database				
$\rho_d$	1	1/2	1/3	1/4	1/5	1/6	1/7	1	3/4	2/3	1/2	1/3
L2	71.33	24.91	6.29	3.51	2.42	1.14	0.72	13.34	4.39	3.16	3.28	2.19
L2-L2	11.36	6.85	4.13	2.40	2.32	2.22	1.69	3.75	3.04	3.10	2.58	1.99
PGH	5559.53	4863.18	2195.03	1383.28	822.11	627.95	383.86	5229.75	2812.96	2178.91	1324.59	557.65
BOMP	139.69	99.88	98.05	89.83	89.95	90.41	87.60	108.52	98.84	98.60	97.25	95.58
BMPL	39.72	17.05	12.94	7.86	7.62	6.53	6.19	14.29	10.87	10.20	7.14	4.57
#speedup	140.0	<b>283.6</b>	169.6	176.0	107.9	96.2	62.0	<b>366.0</b>	258.8	213.6	185.5	122.0

TABLE VII  
AVERAGE SPARSITY ON TWO FACE DATABASES

	Extended YaleB Database							AR Database				
$\rho_d$	1	1/2	1/3	1/4	1/5	1/6	1/7	1	3/4	2/3	1/2	1/3
BOMP	200	200	200	200	200	200	200	200	200	200	200	200
PGH	164	165	165	162	156	158	163	133	130	127	135	124
BMPL	167	165	160	155	155	149	143	189	190	188	194	201

has been developed to vastly speed up SR with many signals. Comprehensive experiments demonstrate the superb efficiency of the proposed (S)MPL methods. In general, (S)MPL are tens times faster than state-of-the-art  $\ell_1$ -norm methods. The recovery time of the SMPL method over a *Big Dictionary* with one million atoms is less than 50 seconds. We apply BMPL to batch face recognition tasks. The experimental results show that BMPL achieves significantly better recognition rates than L2 and L2-L2 with comparable computational cost. Notably, BMPL is up to 20 times faster than the batch-mode OMP [24] and 400 times faster than the  $\ell_1$ -norm methods considered to be state-of-the-art.

#### ACKNOWLEDGEMENT

The authors would like to thank the anonymous reviewers for their insightful comments and suggestions which have greatly improved the paper. This research was partially supported by the Australian Research Council Future Fellowship FT130100746, Australian Research Council grants DE120101161, and DP140102270.

#### REFERENCES

- [1] M. Tan, I. Tsang, and L. Wang, "Matching pursuit LASSO Part I: Sparse recovery over big dictionary," Tech. Rep., 2013.
- [2] E. J. Candès and T. Tao, "Decoding by linear programming," *IEEE Trans. Info. Theory*, vol. 51, no. 12, pp. 4203–4215, 2005.
- [3] D. Donoho, "Compressed sensing," *IEEE Trans. Info. Theory*, vol. 52, no. 4, pp. 1289–1306, 2006.
- [4] M. F. Duarte and Y. C. Eldar, "Structured compressed sensing: From theory to applications," *IEEE Trans. Signal Process.*, vol. 59, no. 9, pp. 4053–4085, 2011.
- [5] T. T. Do, L. Gan, N. H. Nguyen, and T. D. Tran, "Fast and efficient compressive sensing using structurally random matrices," *IEEE Trans. Signal Process.*, vol. 60, no. 1, pp. 139–154, 2012.
- [6] J. Mairal, M. Elad, and G. Sapiro, "Sparse representation for color image restoration," *IEEE Trans. Image Process.*, vol. 17, no. 1, pp. 53–69, 2008.
- [7] J. Wright, A. Yang, A. Ganesh, S. Sastry, and Y. Ma, "Robust face recognition via sparse representation," *IEEE Trans. Pattern Anal. Mach.*, vol. 31, no. 2, pp. 210–227, 2009.
- [8] E. Elhamifar and R. Vidal, "Sparse subspace clustering," in *CVPR*, 2009.
- [9] A. Adler, M. Elad, and Y. Hel-Or, "Fast subspace clustering via sparse representations," Department of Computer Science, Technion, Israel, Tech. Rep., 2011.
- [10] A. Coates and A. Ng, "The importance of encoding versus training with sparse coding and vector quantization," in *ICML*, 2011.
- [11] T. Peleg, Y. Eldar, and M. Elad, "Exploiting statistical dependencies in sparse representations for signal recovery," *IEEE Trans. Signal Process.*, vol. 60(5), pp. 2286–2303, 2012.
- [12] G. Davis, S. Mallat, and M. Avellaneda, "Adaptive greedy approximations," *Constr. Approx.*, vol. 13, no. 1, pp. 57–98, 1997.
- [13] D. Ge, X. Jiang, and Y. Ye, "A note on the complexity of lp minimization," *Math. Programming*, vol. 129, no. 2, pp. 285–299, 2011.
- [14] B. Efron, T. Hastie, I. Johnstone, and R. Tibshirani, "Least angle regression," *Ann. Statist.*, vol. 32, no. 2, pp. 407–499, 2004.
- [15] H. Lee, A. Battle, R. Raina, and A. Y. Ng, "Efficient sparse coding algorithms," in *NIPS*, 2006.
- [16] S.-J. Kim, K. Koh, M. Lustig, S. Boyd, and D. Gorinevsky, "An interior-point method for large-scale  $\ell_1$ -regularized least squares," *IEEE J. Sel. Top. Sign. Proces.*, vol. 1, no. 4, pp. 606–617, 2007.
- [17] M. A. T. Figueiredo, R. D. Nowak, and S. J. Wright, "Gradient projection for sparse reconstruction: Application to compressed sensing and other inverse problems," *IEEE J. Sel. Top. Sign. Proces.: Special Issue on Convex Optimization Methods for Signal Processing*, 2007.
- [18] L. Xiao and T. Zhang, "A proximal-gradient homotopy method for the  $\ell_1$ -regularized least-squares problem," in *ICML*, 2012.
- [19] —, "A proximal-gradient homotopy method for the sparse least-squares problem," *SIAM J. Optimiz.*, vol. 23, no. 2, pp. 1062–1091, 2013.
- [20] B. Efron, T. Hastie, L. Johnstone, and R. Tibshirani, "Least angle regression," *Ann. Statist.*, vol. 32, no. 2, pp. 407–499, 2004.
- [21] Y. Nesterov, "Gradient methods for minimizing composite objective function," Center for Operations Research and Econometrics (CORE), Catholic University of Louvain (UCL), Tech. Rep., 2007.
- [22] A. Beck and M. Teboulle, "A fast iterative shrinkage-thresholding

- algorithm for linear inverse problems,” *SIAM J. on Imaging Sciences*, vol. 2, no. 1, pp. 183–202, 2009.
- [23] S. Yun and K.-C. Toh, “A coordinate gradient descent method for  $\ell_1$ -regularized convex minimization,” *Comput. Optim. Appl.*, vol. 48, no. 2, pp. 273–307, 2011.
- [24] R. Rubinstein, M. Zibulevsky, and M. Elad, “Efficient implementation of the  $k$ -SVD algorithm using batch orthogonal matching pursuit,” Technion, Tech. Rep., 2008.
- [25] A. Yang, A. Ganesh, Y. Ma, and S. Sastry, “Fast  $\ell_1$ -minimization algorithms and an application in robust face recognition: A review,” in *ICIP*, 2010.
- [26] R. Baraniuk, “Compressive sensing,” *IEEE Signal Processing Mag.*, vol. 24, no. 4, pp. 118–121, 2007.
- [27] J. Romberg, “Imaging via compressive sampling,” *IEEE Signal Processing Magazine*, vol. 25, no. 2, pp. 14–20, 2008.
- [28] M. Aharon, M. Elad, and A. Bruckstein, “The  $k$ -SVD: An algorithm for designing of overcomplete dictionaries for sparse representation,” *IEEE Trans. Signal Process.*, vol. 54, no. 11, pp. 4311–4322, 2006.
- [29] H. Lee, A. Battle, R. Raina, and A. Y. Ng., “Efficient sparse coding algorithms,” in *NIPS*, 2006, pp. 801–808.
- [30] S. Gao, I. W. Tsang, and L. Chia, “Sparse representation with kernels,” *IEEE Trans. Image Process.*, vol. 22, no. 2, pp. 423–434, 2013.
- [31] W. Deng, J. Hu, and J. Guo, “Extended SRC: Undersampled face recognition via intraclass variant dictionary,” *IEEE Trans. Pattern Anal. Mach.*, vol. 34, no. 9, pp. 1864–1870, 2012.
- [32] L. Zhuang, A. Y. Yang, Z. Zhou, S. S. Sastry, and Y. Ma, “Single-sample face recognition with image corruption and misalignment via sparse illumination transfer,” in *CVPR*, 2013.
- [33] Q. Shi, A. Eriksson, A. v. d. Hengel, and C. Shen, “Is face recognition really a compressive sensing problem?” in *CVPR*, 2011.
- [34] L. Zhang, M. Yang, and X. Feng, “Sparse representation or collaborative representation: Which helps face recognition?” in *ICCV*, 2011.
- [35] G. Huang, H. Jiang, K. Matthews, and P. Wilford, “Lensless imaging by compressive sensing,” in *ICIP*, 2013.
- [36] J. Mairal, F. Bach, J. Ponce, and G. Sapiro, “Online dictionary learning for sparse coding,” in *ICML*. ACM, 2009, pp. 689–696.
- [37] —, “Online learning for matrix factorization and sparse coding,” *JMLR*, vol. 11, pp. 19–60, 2010.
- [38] R. Rubinstein, T. Peleg, and M. Elad, “Analysis  $k$ -SVD: A dictionary-learning algorithm for the analysis sparse model,” *IEEE Trans. Signal Process.*, vol. 61, no. 3, pp. 661–677, 2013.
- [39] B. Beckermann and A. B. J. Kuijlaars, “Superlinear convergence of conjugate gradients,” *SIAM J. Numer. Anal.*, vol. 39, no. 1, pp. 300–329, 2002.
- [40] Y. C. Pati, R. Rezaifar, and P. Krishnaprasad, “Orthogonal matching pursuit: Recursive function approximation with applications to wavelet decomposition,” in *The Twenty-Seventh Asilomar Conference on Signals, Systems and Computers*. IEEE, 1993, pp. 40–44.
- [41] J. A. Tropp, “Greed is good: Algorithmic results for sparse approximation,” *IEEE Trans. Info. Theory*, vol. 50, no. 10, pp. 2231–2242, 2004.
- [42] D. L. Donoho, Y. Tsaig, I. Drori, and J. L. Starck, “Sparse solution of underdetermined systems of linear equations by stagewise orthogonal matching pursuit,” *IEEE Trans. Info. Theory*, vol. 58, no. 2, pp. 1094–1121, 2012.
- [43] T. Blumensath and M. E. Davies, “Stagewise weak gradient pursuits,” *IEEE Trans. Signal Process.*, vol. 57, no. 11, pp. 4333–4346, 2009.
- [44] D. Needell and J. Tropp, “CoSaMP: Iterative signal recovery from incomplete and inaccurate samples,” *Appl. Comput. Harmon. Anal.*, vol. 26, no. 3, pp. 301–321, 2009.
- [45] W. Dai and O. Milenkovic., “Subspace pursuit for compressive sensing signal reconstruction,” *IEEE Trans. Info. Theory*, vol. 55, no. 5, pp. 2230–2249, 2009.
- [46] P. Jain, A. Tewari, and I. S. Dhillon, “Orthogonal matching pursuit with replacement,” in *NIPS*, 2011.
- [47] J. K. Bradley, A. Kyrola, D. Bickson, and C. Guestrin., “Parallel coordinate descent for  $\ell_1$ -regularized loss minimization,” in *ICML*, 2011.
- [48] Z. J. Xiang, H. Xu, and P. J. Ramadge., “Learning sparse representations of high dimensional data on large scale dictionaries,” in *NIPS*, 2012.
- [49] D. Needell and R. Vershynin, “Uniform uncertainty principle and signal recovery via regularized orthogonal matching pursuit,” *J. Found. Comput. Math.*, vol. 9, no. 3, pp. 317–334, 2009.
- [50] T. Blumensath and M. E. Davies, “Iterative hard thresholding for compressed sensing,” *Appl. Comput. Harmon. Anal.*, vol. 27, no. 3, pp. 265–274, 2009.
- [51] T. Blumensath, “Accelerated iterative hard thresholding,” *Signal Process.*, vol. 92, no. 3, pp. 752–756, 2011.
- [52] R. Giryes and M. Elad, “RIP-based near-oracle performance guarantees for subspace-pursuit, CoSaMP, and iterative hard-thresholding,” *IEEE Trans. Signal Process.*, vol. 60, no. 3, pp. 1465–1468, 2012.
- [53] Y. Taigman and L. Wolf, “Leveraging billions of faces to overcome performance barriers in unconstrained face recognition,” Facebook AI Research, Tech. Rep., 2011, arXiv:1108.1122.
- [54] A. Martinez and R. Benavente, “The AR face database,” CVC Tech, Tech. Rep., 1998.